Received: 27 March 2023 | Revised: 17 August 2023 | Accepted: 4 September 2023

DOI: 10.1111/all.15897

Allergy EUROPEAN JOURNAL OF ALLERGY AND CLINICAL IMMUNOLOGY EAACI WILEY

ORIGINAL ARTICLE

Influence of antigen density and TLR ligands on preclinical efficacy of a VLP-based vaccine against peanut allergy

Pascal S. Krenger[1,2,3] | Romano Josi[1,2,3] | Jan Sobczak[1,2,3] | Thalia L. C. Velazquez[4] | Ina Balke[5] | Murray A. Skinner[4] | Matthias F. Kramer[4,6] | Callum J. W. Scott[4] | Simon Hewings[4] | Matthew D. Heath[4] | Andris Zeltins[5,7] | Martin F. Bachmann[1,2,8]

[1]Department of Rheumatology and Immunology, University Hospital of Bern, Bern, Switzerland

[2]Department of BioMedical Research, University of Bern, Bern, Switzerland

[3]Graduate School of Cellular and Biomedical Sciences, University of Bern, Bern, Switzerland

[4]Allergy Therapeutics (UK) Ltd, Worthing, UK

[5]Latvian Biomedical Research and Study Centre, Riga, Latvia

[6]Bencard Allergie GmbH, Munich, Germany

[7]Saiba AG, Zurich, Switzerland

[8]Nuffield Department of Medicine, Centre for Cellular and Molecular Physiology (CCMP), The Jenner Institute, University of Oxford, Oxford, UK

Correspondence
Martin F. Bachmann, Department of Immunology, University Clinic of Rheumatology and Immunology, Inselspital, University of Bern, Bern, Switzerland.
Email: martin.bachmann@me.com

Funding information
Allergy Therapeutics; Schweizerischer Nationalfonds zur Förderung der Wissenschaftlichen Forschung

Abstract

Background: Virus-like particle (VLP) Peanut is a novel immunotherapeutic vaccine candidate for the treatment of peanut allergy. The active pharmaceutical ingredient represents cucumber mosaic VLPs ($CuMV_{TT}$-VLPs) that are genetically fused with one of the major peanut allergens, Ara h 2 ($CuMV_{TT}$-Ara h 2). We previously demonstrated the immunogenicity and the protective capacity of VLP Peanut-based immunization in a murine model for peanut allergy. Moreover, a Phase I clinical trial has been initiated using VLP Peanut material manufactured following a GMP-compliant manufacturing process. Key product characterization studies were undertaken here to understand the role and contribution of critical quality attributes that translate as predictive markers of immunogenicity and protective efficacy for clinical vaccine development.

Method: The role of prokaryotic RNA encapsulated within VLP Peanut on vaccine immunogenicity was assessed by producing a VLP Peanut batch with a reduced RNA content (VLP Peanut low RNA). Immunogenicity and peanut allergen challenge studies were conducted with VLP Peanut low RNA, as well as with VLP Peanut in WT and TLR 7 KO mice. Furthermore, mass spectrometry and SDS-PAGE based methods were used to determine Ara h 2 antigen density on the surface of VLP Peanut particles. This methodology was subsequently applied to investigate the relationship between Ara h 2 antigen density and immunogenicity of VLP Peanut.

Results: A TLR 7 dependent formation of Ara h 2 specific high-avidity IgG antibodies, as well as a TLR 7 dependent change in the dominant IgG subclass, was observed following VLP Peanut vaccination, while total allergen-specific IgG remained relatively unaffected. Consistently, a missing TLR 7 signal caused only a weak decrease in allergen tolerability after vaccination. In contrast, a reduced RNA content for VLP Peanut resulted in diminished total Ara h 2 specific IgG responses, followed by a significant impairment in peanut allergen tolerability. The discrepant effect on allergen tolerance caused by an absent TLR 7 signal versus a reduced RNA content is explained by the observation that VLP Peanut-derived RNA not only stimulates TLR 7 but also TLR 3. Additionally, a strong correlation was observed between the number of Ara h 2

antigens displayed on the surface of VLP Peanut particles and the vaccine's immunogenicity and protective capacity.

Conclusions: Our findings demonstrate that prokaryotic RNA encapsulated within VLP Peanut, including antigen density of Ara h 2 on viral particles, are key contributors to the immunogenicity and protective capacity of the vaccine. Thus, antigenicity and RNA content are two critical quality attributes that need to be determined at the stage of manufacturing, providing robust information regarding the immunogenicity and protective capacity of VLP Peanut in the mouse which has translational relevance to the human setting.

KEYWORDS
allergy treatment, food allergy, immunotherapy vaccines and mechanisms, vaccines

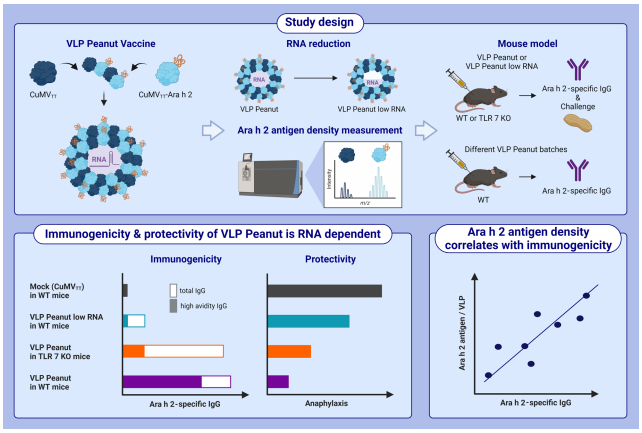

GRAPHICAL ABSTRACT

Virus-like particle (VLP) Peanut is a novel immunotherapeutic vaccine candidate for the treatment of peanut allergy. Encapsulated prokaryotic RNA is a key contributor to the immunogenicity and protective capacity of the VLP Peanut vaccine. Antigen density of Ara h 2 on the particle surface positively correlates with the immunogenicity of the VLP Peanut vaccine. Abbreviations: CuMV, cucumber mosaic virus; IgG, immunoglobulin G; KO, knock out; RNA, ribonucleic acid; TLR, toll-like receptor; TT, tetanus toxin epitope; VLP, virus-like particle; WT, wild type.

1 | INTRODUCTION

Virus-like particles (VLPs) are an excellent vaccine platform since their characteristics combine safety with high immunogenicity.[1] As of today, several VLP-based vaccines are available on the market, such as Cervarix®, Gardasil®, and Gardasil 9® against human papilloma virus (HPV) or Engerix B® against Hepatitis B Virus (HBV).[2] The extraordinary immunogenicity of VLPs is caused by their close resemblance to real viruses which is reflected by sharing the following pathogen-associated molecular (PAMPs) and structural patterns (PASPs): their repetitive structure and nano-size, as well as packaged nucleic acids. The latter is not pathogenic genetic material, but rather nucleic acids derived from the host cell expression system randomly co-packaged during VLP assembly.[3]

Viruses are usually of a spherical, helical or rod-like structure. This is due to the fact that viruses, especially RNA viruses, do not have the space within their small genome to encode for a large variety of structural proteins. As a consequence, viral surfaces are made of a single or, at most, a few different coat proteins ending up in a highly repetitive surface structure.[4,5] The same holds true for VLPs, as they are usually generated by the expression of one or a few viral envelope or coat proteins.[3] In the course of evolution, the host's immune system has learned to recognize and react to particles bearing such PASPs.[6] Thus, binding and cross-linking of the B cell receptor (BCR) through highly repetitive objects is sufficient to induce a strong B cell activation signal, even in the absence of T cells.[7] Particles having characteristic PASPs are also easily recognized by the complement system leading to enhanced B cell activation via binding of CD21 causing engagement of the co-stimulatory molecule CD19[8] and binding to follicular dendritic cells. Moreover, complement bound particles are preferably taken up by antigen presenting cells (APCs) facilitating T-cell priming.[9] Accordingly, PASP bearing particles, such as viruses or VLPs, are exemplary for the induction of a strong humoral response. The geometry underlying PASP is thereby not free of regularity, but rather dependent on certain determinants. One of these determinants was found to be the distance of one

antigen to the other on the viral surface, also referred as antigen density. Using haptenated polymers, it was previously shown that 15–20 hapten-molecules that are 5–10 nm aside from each were shown to be optimal for B cell activation.[10] Interestingly, the average distance between viral coat proteins is within this range, thereby affirming this observation.[4]

VLPs do not contain any pathogenic genetic material. However, VLPs derived from RNA viruses can carry RNA derived from the host cell expression system.[3] Based on their negative charge, these nucleic acids provide stability to the particle and are essential for particle assembly.[11] For reasons of electrostatic interaction with the coat proteins, the amount of encapsulated RNA is usually similar in size to the virion of the virus from which the VLP is derived.[12,13] As ligands for Toll-like receptors (TLRs), the VLP-carried RNA is thereby not only of structural but also of immunological significance. TLRs belong to the pattern recognition receptors (PRRs) and as such, they are responsible for sensing pathogen-associated molecular patterns (PAMPs). TLR signaling initiates the transcription of pro-inflammatory cytokines and Type I interferons, orchestrating the recruitment and activation of innate immune cells.[14,15] However, TLR signaling is not exclusive to the innate immune system, since B cells also express TLRs and are stimulated by TLR ligands.[16] Prokaryotic derived single- and double-stranded RNA (ssRNA and dsRNA), acting as TLR 7/8, respectively TLR 3 ligands, are commonly packaged into VLPs during the process of assembly.[3,16] This is of major importance, especially for the type of humoral immune response induced by VLP vaccination. For example, isotype switching to IgG2a/c and IgG2b after VLP-vaccination was shown to be conditional on BCR engagement in combination with TLR signaling. Abolishing TLR signaling in B cells prevented switching to these IgG subclasses, demonstrating the B cell intrinsic nature of this process.[17,18] Furthermore, TLR 7 signaling in particular was necessary for the generation of potent secondary plasma cells out of memory B cells.[19] Enhanced B cell proliferation, increased BCR hypermutation, as well as enhanced BCR repertoire diversity, were observed in relation to B cell intrinsic TLR signaling.[20–22] Consequently, TLR signaling significantly contributes to the quality of the induced immune response and brings TLR ligands into the focus of VLP-vaccine design and development to induce protective, high affinity, and long-lived antibody responses.

In the present study, TLR signaling is monitored to investigate the role of encapsulated RNA within a VLP (i.e., VLP-carried RNA), including the role of antigen density, following vaccination with VLP Peanut. VLP Peanut is a promising vaccine candidate for the treatment of peanut allergy. The active substance represents VLPs comprised of capsid subunit proteins (cucumber mosaic virus [CuMV] engineered with a universal T cell epitope derived from the tetanus toxin [TT] i.e., $CuMV_{TT}$) and the peanut allergen (Ara h 2) capsid fusion protein ($CuMV_{TT}$-Ara h 2). Upon co-expression of $CuMV_{TT}$ and $CuMV_{TT}$-Ara h 2 genes in *Escherichia coli* (*E. coli*), mosaic VLPs form around prokaryotic RNA, thereby comprising VLP Peanut.[23–25] Previous studies conducted by Storni et al.[23] and Sobczak et al.[25] revealed that $CuMV_{TT}$-based vaccination targeting the single allergens Ara h 1 or Ara h 2 mediates protection against anaphylaxis induced by complex peanut allergen mixtures in mice. Vaccine induced protection is thereby dependent on the allergen-specific IgG antibodies neutralizing the allergen, promoting IgE internalization by mast cells as well as engaging the inhibitory receptor FcγRIIb present on mast cells and basophils.[23,25–27] Importantly, allergens displayed in viral fashion fail to activate human mast cells, demonstrating the safety of VLP vaccination for allergy treatment.[28]

The objective of this study was to assess the biological role of key quality attributes of the VLP Peanut vaccine such as prokaryotic RNA and Ara h 2-antigen content at the development stage of manufacture. Information gained in this context on the immunogenicity and protective capacity of different batch variants facilitated the development of a control strategy that allowed the establishment of a reproducible cGMP-certified production process. Specifically, we observed a TLR 7-dependent formation of Ara h 2 specific high-avidity IgG and IgG2c subclass antibodies after VLP Peanut vaccination in mice. However, the absence of TLR 7 stimulation had little effect on the formation of total Ara h 2 specific IgG antibodies and, for this reason, only slightly reduced the tolerance to peanut allergen in peanut-allergic mice immunized with VLP Peanut. In contrast, vaccination with VLP Peanut carrying reduced amounts of RNA led to a dramatic decrease in Ara h 2-specific IgG antibodies and significantly reduced resistance to peanut allergen challenge in peanut allergic mice, likely explained by reduced TLR 3 stimulation. Furthermore, a clear correlation between the Ara h 2 antigen density displayed on $CuMV_{TT}$ particles and VLP Peanut vaccine immunogenicity could be shown. As such, RNA content and antigen density for VLP Peanut are identified here as critical contributors to vaccine immunogenicity and protectivity.

2 | MATERIALS AND METHODS

2.1 | Mice

In vivo experiments were conducted in 8-week-old female C57BL/6 wild-type mice purchased from Envigo or in 8-week-old female TLR 7 knock-out (B6.129P2-Tlr7tm1Aki) mice kindly donated from Prof. Dr. Pål Johansen. Animal procedures were performed in accordance with the Swiss Animal Act (455.109.1—September 5, 2008) at the DBMR of the University of Bern. All animal experiments were conducted by protocols approved by the Cantonal Veterinary Office Bern, Switzerland (License BE79/2021).

2.2 | $CuMV_{TT}$, VLP Peanut, and VLP Peanut low RNA production and purification

Expression and purification of $CuMV_{TT}$ was described in detail in Zeltins et al.[24] VLP Peanut expression and purification was described in detail in Sobczak et al.[25] VLP Peanut low RNA was produced as follows. VLP Peanut at a concentration of 1.5 mg/mL was derivatized by

the addition of succinimidyl 6-(beta-maleimidopropionamido) hexanoate (SMPH; Thermo Fisher Scientific, Cat. 22363) at 10 times molar excess to VLP Peanut for 30 min at 25°C. Unreacted SMPH was removed by buffer exchange on Amicon-Ultra-0.5, 100 K filtration units (Millipore, Cat. UFC510024) four times with 5 mM Na phosphate pH 7.5, 2 mM EDTA buffer. RNase A (Roche, Cat. 10109169001) was added in 5 µg/mL final concentration, and the sample was incubated at room temperature for 1 week. Reduction of VLP Peanut carried RNA was quantified by using the Qubit™ RNA BR Assay Kit (Thermo Fisher Scientific, Cat. Q10210). Obtained results were confirmed by loading 15 µL sample (1 mg/mL) mixed with 2.5 µL loading dye (New England BioLabs, Cat. B7024S) onto a 1% Agarose (BioConcept, 7-01P02-R) gel, run in Tris-borate-EDTA (TBE) buffer at 50 V. Gel picture was taken with Azure Biosystems c300 using the UV302 channel, exposure time 10 s. DNA Ladder (Thermo Scientific, Cat. SM0242) was included in the agarose analysis. Signal intensity of RNA derived band on agarose gel picture was quantified with FIJI Image J software v1.53c.[29] Additional batches were produced in fermenters and purified using various strategies to optimize cGMP-certified production. Batches differed with respect to size and purification strategies during pharmaceutical development, forming an integral part in developing reproducible cGMP-certified production. Endotoxin content of each batch was below 100 EU per vaccine dose.

2.3 | Transmission electron microscopy (TEM)

Physical integrity of VLP vaccine batches was confirmed by transmission electron microscopy (Philips CM12 EM). To this end, sample grids were glow discharged and 10 µL of VLP sample (1 mg/mL) was added for 30 s. Grids were washed three times with ddH_2O and negatively stained with 5 µL of 5% uranyl acetate for 30 s. Excess uranyl acetate was removed by pipetting, and the grids were air-dried for 10 min. Images were taken with 84,000× and 110,000× magnification.

2.4 | Dynamic light scattering (DLS)

Average VLP particle size in vaccine batches was measured by DLS using the Zetasizer Nano ZS instrument (Malvern Panalytical Ltd), and measurements were evaluated with DTS software v. 6.32 (Malvern Panalytical Ltd). Three consecutive measurements were performed per sample.

2.5 | Vaccination regimen for naïve mice

Mice were vaccinated subcutaneously (s.c.) with 30 µg vaccine in 100 µL PBS by the usage of an insulin syringe (B Braun Omnican®, Cat. 9151133S). A booster injection with an equal dose was performed 21 and 42 days post prime. Serum was collected before prime and 56 days post prime via tail bleeding and serum was isolated using BD Microtainer® Collection Tube (BD Biosciences, Cat. 365967). Immunogenicity studies were performed with five mice per group. Deviating from this, groups of four mice were used for $CuMV_{TT}$ control and VLP Peanut batch 2 in the immunogenicity study investigating the correlation of Ara h 2 antigen density and immunogenicity.

2.6 | Challenge of peanut sensitized and vaccinated mice

Naïve mice were sensitized to peanut by giving 5 µg non-roasted peanut extract (Ara N) in 200 µL Alhydrogel® (10 mg/mL $Al(OH)_3$; InvivoGen, Cat. vac-alu-250) intraperitoneally (i.p.) twice in a 7-day interval.[23,25,30] Ara N peanut extract was obtained by following the protocol from Koppelmann et al.[23] Mice were vaccinated s.c. with 30 µg vaccine 14 days after sensitization. Subsequently, two booster injections with an equal dose were performed at 21-day intervals. Fourteen days after the last booster injection mice were challenged with 20 µg Ara N peanut extract given i.v. in 100 µL PBS by the usage of an insulin syringe (B Braun Omnican®, Cat. 9151133S). Body core temperature was measured in 10 min intervals for 1 h with Mini Temp Veterinary Temperature Monitor (Vetronic Services LTD, Cat. MTEMP). Challenge studies were performed with six mice per WT and five mice per TLR 7 KO group.

2.7 | Enzyme-linked immunosorbent assay (ELISA)

Recombinant Ara h 2 protein was produced as described in Storni et al.[23] For the determination of Ara h 2 and $CuMV_{TT}$ specific IgG antibodies found in serum of vaccinated mice an ELISA experiment was performed as follows. ELISA plates (CORNING, Cat. 3690) were coated with recombinant Ara h 2 or $CuMV_{TT}$ diluted in PBS to a concentration of 1 µg/mL (50 µL per well) and incubated overnight at 4°C. ELISA plates were washed with 100 µL PBS per well for four times with Microplate washer (BioTek 405 TS Microplate Washer, Agilent) and blocked afterward by the addition of 100 µL PBS-Casein 0.15% per well for 2 h at room temperature. Plates were flicked and mouse serum was added. 1:20 or 1:10 pre-diluted sera were serially diluted 1:3 on the plate in PBS-Casein 0.15% in a total volume of 50 µL, incubated for 1.5 h at room temperature. After washing with 100 µL PBS-0.01% Tween for four times with microplate washer, goat anti-mouse IgG conjugated to horseradish peroxidase (HRP) (Jackson ImmunoResearch, Cat. 115–035-071) was added at 1:1000 dilution in PBS-Casein 0.15% (50 µL per well) and the plate incubated for another hour at room temperature. ELISA plates were washed with 100 µL PBS-0.01%Tween for four times with Microplate washer and 50 µL per well of developing solution (30 mM Citratbuffer including 5% tetramethylbenzidine and 1.5 ‰ H_2O_2) was added. The color reaction was stopped by the addition of 50 µL per well of 1 M H_2SO_4 and absorbance at 450 nm (OD_{450}) was read with BioTek Cytation 5 imaging reader. Half-maximal antibody titers (OD_{50}) were defined as the reciprocal of the dilution leading to half of the OD measured at saturation.

IgG subclass antibody titers were determined following the same procedure with a different detection antibody: Rat anti-mouse IgG1 HRP (BD Pharmingen, Cat. 559626, 1:1000 dilution), goat anti-mouse IgG2c HRP (Southern BioTech, Cat No 1078–05, 1:1000 dilution), goat anti-mouse IgG2b HRP (Invitrogen, Cat. M32407, 1:1000 dilution).

2.8 | Avidity ELISA

High-avidity IgG antibodies were determined by a previously described protocol.[31] To this end, the ELISA protocol described above was extended by one additional step. Two plates similarly coated and incubated with the same sera were washed upon sera incubation either for three times with PBS-0.01%Tween or with 7 M urea in PBS-0.01%Tween for 5 min at room temperature (50 µL per well). After this additional washing step, goat anti-mouse IgG conjugated to HRP (Jackson ImmunoResearch, Cat. 115-035-071) was added at 1:1000 dilution in PBS-Casein 0.15% (50 µL per well) and the protocol described above continued. The avidity index (AI) was calculated by AIx = (OD_{450} (dilution x) + urea)/(OD_{450} (dilution x) − urea).

2.9 | HEK-Blue™ TLR 3/7 cell assay

RNA encapsulated within VLP Peanut was isolated as follows. VLPs and TRIzol® agent (Invitrogen, Cat. 15596026) were mixed and incubated for 10 min on ice in a mass to volume ratio (m_{VLP}/v_{TRIzol}) of 1/1.25. Subsequently, samples were centrifuged for 10 min at 12,000 g at 4°C. The supernatant was mixed with chloroform at a ratio of 1/0.25 ($m_{VLP}/v_{chloroform}$) and incubated for 10 min on ice, then centrifuged for 15 min at 12,000 g at 4°C. The upper phase was mixed with isopropanol at a ratio of 1/0.6 ($m_{VLP}/v_{isopropanol}$) and incubated for 10 min on ice, then centrifuged for 10 min at 12,000 g at 4°C. The pellet was washed with 75% EtOH and afterward resuspended in 100 µL DEPC water (Invitrogen, Cat. AM9906). RNA concentration was measured with NanoDrop™ 1000 (Thermo Scientific). Size distribution of isolated RNA was analyzed by a 1% Agarose gel (BioConcept, 7-01P02-R) run in MOPS buffer (3-(N-morpholino)propanesulfonic acid). RNA ladder (Thermo Scientific, Cat. #SM1821) was included into analysis. TLR 3 and TLR 7 stimulation capacity of RNA isolated from VLP Peanut was determined by HEK-Blue™ hTLR 3 (InvivoGen, Cat. hkb-htlr3) and HEK-Blue™ hTLR 7 (InvivoGen, Cat. hkb-htlr7) cell assay following the manufacturer's instructions. Thereby, 50,000 cells (TLR 3) or 40,000 cells (TLR 7) were stimulated in triplicates with 250, 500, and 1000 ng of isolated RNA or 20 ng of positive control (poly(I:C) HMW for TLR 3, CL264 for TLR 7). TLR 3/7 stimulation capacity of RNA isolated out of VLP Peanut was normalized to positive control stimulated cells.

2.10 | Mass spectrometry

For each sample, 50 µg of protein were precipitated with trichloroacetic acid (TCA; Sigma-Aldrich) at a final concentration of 5% and washed twice with ice-cold acetone. Samples were resuspended in 50 mM TEAB (Triethylammonium bicarbonate), and 20 µg were reduced with 2 mM TCEP (tris(2-carboxyethyl)phosphine) and alkylated with 15 mM Chloroacetamide at 30°C for 30 min. Proteins were digested with 500 ng of sequencing-grade Lys C (Wako Chemicals) for 2 h at 37°C, before adding 500 ng of sequencing-grade Glu C (Roche) for overnight digestion at 37°C. The samples were dried to completeness and re-solubilized in 20 µL of MS sample buffer (3% acetonitrile, 0.1% formic acid). Peptide concentration was determined using the Lunatic UV/Vis polychromatic spectrophotometer (Unchained Labs). Samples were diluted to an absorbance value of 0.004 (A280) and spiked with 50 fmol/µL stable-isotope labelled peptides (see below). For determination of peptide suitability, a pooled sample was serially diluted 1:2 for a final of six different concentrations. Maxi SpikeTides QL_AAA were synthesized at >95% purity by JPT Peptide Technology GmbH as determined by HPLC, MS, and amino acid analysis. C-terminal Lysines or internal Arginines or Valines were incorporated as heavily labelled amino acids (Arg: U-13C6, U-15 N4; Lys: U-13C6, U-15 N2; Val: U-13C5, U-15 N).

Mass spectrometry analysis was performed on an Orbitrap Exploris 480 mass spectrometer (Thermo Fisher Scientific) equipped with a Nanospray Flex Ion Source (Thermo Fisher Scientific) and coupled to an M-Class UPLC (Waters). Solvent composition at the two channels was 0.1% formic acid for channel A and 0.1% formic acid, 99.9% acetonitrile for channel B. Column temperature was 50°C. For each sample 1 µL of peptides spiked with heavy labeled standard peptides were loaded on a commercial nanoEase MZ Symmetry C18 Trap Column (100 Å, 5 µm, 180 µm × 20 mm, Waters) followed by a nanoEase MZ C18 HSS T3 Column (100 Å, 1.8 µm, 75 µm × 250 mm, Waters). The peptides were eluted at a flow rate of 300 nL/min. After a 3 min initial hold at 5% B, a gradient from 5% to 35% B in 60 min was applied. The column was cleaned after the run by increasing to 95% B and holding 95% B for 10 min prior to re-establishing loading condition for another 10 minutes.

For MS2-based absolute quantification, the mass spectrometer was operated in targeted MS mode (tMS) with a scheduled inclusion list (5 min windows) of the indicated peptides (light and heavy) and charge states using Xcalibur 4.4 (Tune version 3.1.279.9), with spray voltage set to 2.7 kV, funnel RF level at 40%, heated capillary temperature at 275 °C, and advanced peak determination (APD) on. Full-scan MS spectra (350–1′500 m/z) were acquired at a resolution of 120,000 at 200 m/z after accumulation to a target value of 3,000,000 or for a maximum injection time of 50 ms. Target ions were isolated using a quadrupole mass filter with 1 m/z isolation window and fragmented by higher-energy collisional dissociation (HCD) using a normalized collision energy of 30%. HCD spectra were acquired at a resolution of 60,000 and maximum injection time was set to Auto with Loop Control set to All and an automatic gain control (AGC) of 100,000 ions. The samples were acquired using internal lock mass calibration on m/z 371.1012 and 445.1200.

The mass spectrometry proteomics data were handled using the local laboratory information management system (LIMS)[32] and all relevant data have been deposited to the ProteomeXchange Consortium via the PRIDE (http://www.ebi.ac.uk/pride) partner repository with the data set identifier PXDXXXX.

Peptide quantification and manual spectrum annotations were done in Skyline (21.2.0.369) and visualized using RStudio (1.4.1717) and R (4.1.1). In order to generate spectral libraries for the selected peptides, MS data were imported into PEAKS Studio (Bioinformatic Solutions) and searched against a database containing the sequences of the modified and unmodified VLPs as well as a generic *E.coli* database (fgcz_83334_ecoli_O157_20191119). Identity assignments between endogenous and SIL peptides were evaluated by determining spectra similarity via dot product (dotp, value >0.8) measurements against the project library. Endogenous peptide quantification was done by one-point calibration using the spiked in SIL peptide and is given in fmol for each peptide. Ara h 2 specific peptide was normalized to both $CuMV_{TT}$-backbone peptides and the mean of both ratios was defined as Ara h 2 antigen density.

Peptides used for absolute quantification: $CuMV_{TT}$-backbone (RLLLPDS**V**TE, YAVLVYS**K**), Ara h 2-insert (NQSDRLQG**R**QQE), no insert (IDRGSYYG**K**).

2.11 | SDS-PAGE Analysis

Fifteen microlitres of vaccine samples (1 mg/mL) were mixed with 3 µL reducing buffer (Thermo Scientific, Cat. 39000) and heated for 5 min at 95°C prior to loading onto a 12% SDS-PAGE with a 4% stacking gel together with 6 µL protein ladder (Thermo Scientific, Cat. 26616). The gel was run at 70 V in running buffer (Tris (hydroxymethyl)-aminoethane 2.5 mM, Glycine 25 mM, SDS 0.01%) and afterward stained in InstantBlue® Coomassie Protein Stain (Abcam, Cat. Ab119211). Gel picture was taken with Azure Biosystems c300 using the visible channel, exposure time 10 s. Signal intensity of $CuMV_{TT}$-Ara h 2 and $CuMV_{TT}$ derived bands on gel picture was quantified with FIJI Image J software v1.53c.[29] The Ara h 2 antigen density of VLP Peanut batches determined by SDS-PAGE was calculated as follows. Measured protein band intensities of $CuMV_{TT}$-Ara h 2 were divided by corresponding protein band intensities for $CuMV_{TT}$. The different molar masses were thereby taken into account and the obtained quotient multiplied by 180 (total number of subunits per VLP) to obtain the Ara h 2 antigen density per VLP.

2.12 | Statistics

All data are presented as mean ± SEM. Data were analyzed using ordinary one-way ANOVA with Tukey correction for multiple comparisons or using unpaired *t*-test. Pearson correlation coefficient was calculated for the determination of a linear correlation between two sets of data. Analyses were performed using GraphPad PRISM 9.4 (GraphPad Software Inc). The value of $p < 0.05$ was considered statistically significant. Statistical significance is noted in figures as $^{*}p < 0.05$, $^{**}p < 0.01$, $^{***}p < 0.001$, $^{****}p < 0.0001$.

3 | RESULTS

3.1 | Physical integrity of VLP Peanut is not compromised by a 50% reduction of the encapsulated RNA

VLP Peanut was produced by the co-expression of modified $CuMV_{TT}$-Ara h 2 and unmodified $CuMV_{TT}$ genes in *E.coli*. In this process, the expressed $CuMV_{TT}$-Ara h 2 and $CuMV_{TT}$ proteins assemble around the negatively charged prokaryotic RNA thereby spontaneously forming VLPs (Figure 1A).[25] VLPs consisting only of unmodified $CuMV_{TT}$ were produced at the same and served as controls in further experiments.[25] To investigate the role of the carried prokaryotic RNA for the immunogenicity of VLP Peanut we reduced the RNA content in one batch by RNA digestion (VLP Peanut low RNA). To prevent loss of stability caused by reduction of the encapsulated RNA, particle subunits were cross-linked by SMPH prior to RNAse treatment. The correct VLP formation with its characteristic T = 3 icosahedral geometry, which is important for efficient draining into secondary lymphoid organs was confirmed by TEM for VLP Peanut low RNA and VLP Peanut (Figure 1B).[6,33] VLP Peanut low RNA VLPs were slightly larger in size compared with VLP Peanut VLPs (average diameter = 36 nm) (Figure 1B). SDS-PAGE analysis of VLP Peanut and VLP Peanut low RNA revealed preserved incorporation rates of $CuMV_{TT}$-Ara h 2 subunits into VLPs, demonstrating that the RNase treatment did not affect the particle's composition (Figure 1C,D). RNA digestion reduced the amount of the carried RNA by around 50% as measured by Agarose gel analysis (Figure 1E,F) and Qubit™ RNA BR Assay (Figure 1G). Consequently, RNA digestion reduced the amount of VLP Peanut-carried RNA by half without compromising its physical integrity.

FIGURE 1 Physical integrity of VLP Peanut is not compromised by a 50% reduction of the encapsulated RNA. (A) Schematic representation of VLP Peanut ($CuMV_{TT}$/$CuMV_{TT}$-Ara h 2) expression in *E. coli*. created with BioRender.com. (B) TEM and DLS of VLP Peanut low RNA and VLP Peanut, scale bar 200 nm. (C) 12% SDS-PAGE of M. Protein Ladder, C. $CuMV_{TT}$, 1. VLP Peanut low RNA, 2. VLP Peanut. $CuMV_{TT}$-Ara h 2 derived protein bands are circled in orange, $CuMV_{TT}$ derived protein bands in dark blue. (D) Ara h 2 antigen density of C. $CuMV_{TT}$, 1. VLP Peanut low RNA, 2. VLP Peanut determined based on FIJI image J software analysis of protein band intensities from SDS-PAGE depicted in (C). (E) Agarose gel analysis of M_N. Nucleic Acid Ladder, 1. VLP Peanut low RNA, 2. VLP Peanut. (F) Intensity of RNA derived bands depicted in (E) analyzed by FIJI image J software. (G) RNA content of 1. VLP Peanut low RNA, 2. VLP Peanut measured with Qubit™ RNA BR Assay Kit. Statistical analysis (mean ± SEM) using ordinary one-way ANOVA with Tukey correction for multiple comparisons in (D) and unpaired *t*-test in (F and G). $p < 0.05$ (*), $p < 0.0001$ (****). $N = 3$, $N = 2$ for Qubit™ RNA BR Assay.

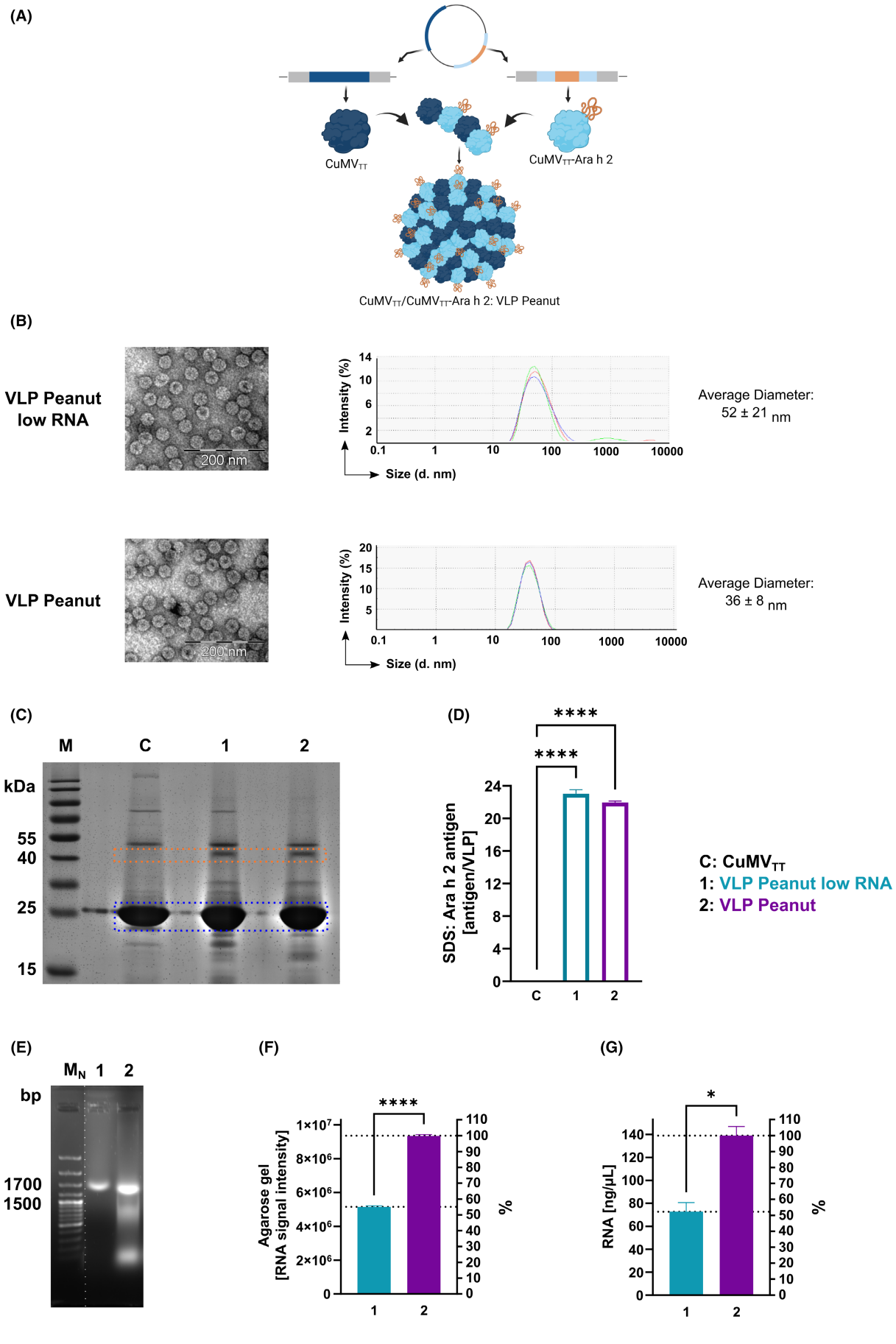

3.2 | Ara h 2 specific total IgG responses are highly dependent on VLP Peanut carried RNA and TLR 7 signaling promotes the formation of high-avidity IgG as well as IgG2b 7 signaling promotes the formation of high-avidity

We examined the role of the VLP Peanut RNA content on the vaccine's immunogenicity profile. Groups of C57/BL6 WT mice were vaccinated s.c. with 30 μg VLP Peanut, VLP Peanut low RNA, or $CuMV_{TT}$ three times in intervals of 21 days. TLR 7 KO mice were immunized with VLP Peanut or VLP Peanut low RNA using the same vaccination regimen. Sera were collected before prime (D0) and 14 days after the second booster injection (D56). Serum IgG antibodies specific for the Ara h 2 antigen or the $CuMV_{TT}$-carrier were determined by ELISA (Figure 2A). Ara h 2 specific IgG titers reached comparable levels in WT and TLR 7 KO mice after VLP Peanut immunization. By contrast, a significant reduction of Ara h 2 specific IgG titers was observed in WT and TLR 7 KO mice immunized with VLP Peanut low RNA. Mice immunized with $CuMV_{TT}$ control did not exhibit Ara h 2 specific IgG antibodies (Figure 2B,C). No Ara h 2 specific IgG antibodies were detected before immunization (Figure S1A). We performed avidity assays by washing ELISA plates with 7 M urea to remove low avidity antibodies. Whereas about 80% of the Ara h 2 specific antibodies in VLP Peanut immunized WT mice were of high-avidity, this value decreased to 20% in VLP Peanut immunized TLR 7 KO mice and was almost 0% in VLP Peanut low RNA immunized WT or TLR 7 KO mice (Figure 2D). A clear pattern in Ara h 2 specific IgG subclass distribution was observed between different groups. IgG2c and IgG2b antibodies were predominantly found in VLP Peanut immunized WT mice. IgG1 antibodies were the main IgG subclass formed in the absence of a TLR 7 stimulus (VLP Peanut immunized TLR 7 KO mice) and VLP Peanut low RNA immunized mice barely developed anti-Ara h 2 IgG subclass antibodies (Figure 2E). Antibodies against the VLP carrier $CuMV_{TT}$ were also measured. $CuMV_{TT}$ specific IgG antibodies were detected to the same extent in all groups including $CuMV_{TT}$ immunized mice (Figure 2F,G). Before immunization, no $CuMV_{TT}$ specific IgG antibodies were found in serum (Figure S1B). Around 40% of $CuMV_{TT}$ specific IgG antibodies were of high-avidity, as they were resistant to washing with 7 M urea (Figure 2H). In general, the anti-$CuMV_{TT}$ IgG subclass distribution was balanced between groups (Figure 2I). Taken together, these data suggest that the Ara h 2 antigen specific IgG immune responses are highly dependent on RNA-derived stimuli, whereas the $CuMV_{TT}$-carrier specific IgG immune responses are less so. Thus, VLP-carried RNA strongly contributes to the immunogenicity of antigens that are less abundant on the VLP surface (Ara h 2 here), compensating for the lower repetitiveness of these antigens and restoring their immunogenic character. The remaining immunogenicity of $CuMV_{TT}$ is indicative for a preserved overall particle structure. Lowering the RNA content of VLP Peanut reduced vaccine immunogenicity for Ara h 2 much more than a missing TLR 7 signal did. This suggests that the observed TLR 3 signal induced by intact RNA (Figure 3) is important for total IgG formation but less so for isotype switching to IgG2c. TLR 7 signaling, however, was linked to high-avidity IgG as well as to IgG2b/c subclass antibody formation. These results indicate the critical role of the VLP-carried RNA and TLR 7 signaling for vaccine immunogenicity.

3.3 | VLP Peanut carried RNA stimulates both TLR 7 and TLR 3

Our immunogenicity study revealed that a low RNA content has a greater impact on Ara h 2 specific IgG responses than a lack of a TLR 7 signal does. We concluded that other TLRs, for example, TLR 3, a sensor for dsRNA, might be involved in the underlying process.[34] To investigate this, HEK-Blue™ TLR 7 and TLR 3 reporter cells were stimulated with 250, 500, and 1000 ng RNA isolated out of VLP Peanut. VLP Peanut derived RNA pointed out a broad distribution in size, with a maximum at around 500 bp (Figure 3A). A dose dependent stimulation by the VLP Peanut derived RNA was observed in equal mass for TLR 3 as well as for TLR 7 reporter cells (Figure 3B,C). This indicates that the bacterial RNA contained in VLP Peanut exists in both single- and double-stranded forms, stimulating TLR 7 and TLR 3 to the same degrees. A missing TLR 7 signal can partially be compensated by a TLR 3 derived signal as both TLRs are expressed in B cells.[35,36] This would explain the weaker effect of an absent TLR 7 signal on VLP Peanut vaccine immunogenicity compared with reduced RNA content.

3.4 | VLP Peanut mediated protection from anaphylaxis depends on encapsulated RNA

Peanut allergy can become a serious health threat as small amounts of peanuts can induce strong allergic reactions.[37,38] Here, we investigated the role of the VLP Peanut carried RNA on the vaccine's systemic protection capacity by following a well-established mouse model for IgE-mediated anaphylaxis upon peanut sensitization.[23,25,30] C57/BL6 WT or TLR 7 KO mice were sensitized to peanut by injecting 5 μg whole peanut extract in 200 μL Alhydrogel® i.p. on Day 0 and 7. Fourteen days later mice were vaccinated

FIGURE 2 Ara h 2 specific total IgG responses are highly dependent on VLP Peanut-carried RNA and TLR 7 signaling promotes the formation of high-avidity IgG as well as IgG2b/c subclass antibodies. (A) Vaccination regimen and bleeding schedule, scheme created with BioRender.com. Ara h 2 specific serum IgG, OD_{450} shown in (B), Log_{10} OD_{50} shown in (C). (D) Avidity index of Ara h 2 specific serum IgG. (E) Ara h 2 specific serum IgG1, IgG2b, and IgG2c, Log_{10} OD_{50} shown. $CuMV_{TT}$ specific serum IgG, OD_{450} shown in (F), Log_{10} OD_{50} shown in (G). (H) Avidity index of $CuMV_{TT}$ specific serum IgG. (I) $CuMV_{TT}$ specific serum IgG1, IgG2b, and IgG2c, Log_{10} OD_{50} shown. Statistical analysis (mean ± SEM) using ordinary one-way ANOVA with Tukey correction for multiple comparisons. $p < 0.05$ (*), $p < 0.01$ (**), $p < 0.001$ (***). $p < 0.0001$ (****). $N = 5$ One representative of two similar experiments is shown.

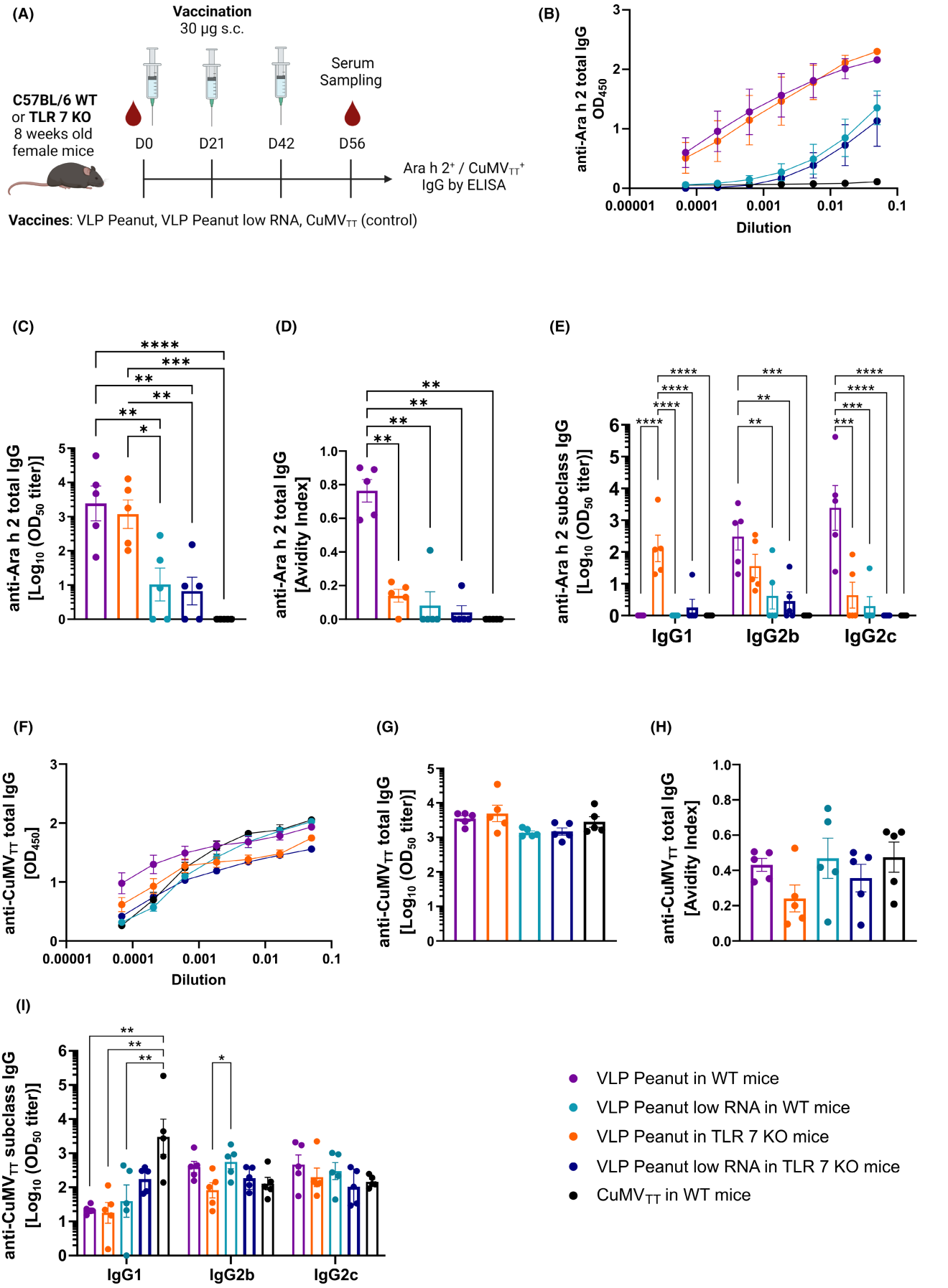

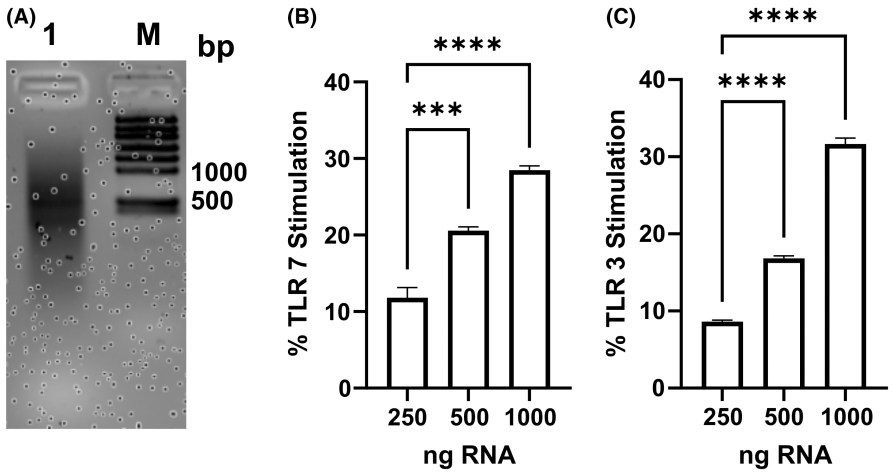

FIGURE 3 VLP Peanut-carried RNA stimulates both TLR 7 and TLR 3. (A) Agarose gel analysis of 1: VLP Peanut-derived RNA, M: RNA Ladder. Dose-dependent TLR 7 (B) and TLR 3 (C) stimulation by RNA isolated out of VLP Peanut determined by HEK-Blue™ TLR 3/7 in vitro assay. Results normalized to positive control stimulated HEK-Blue™ TLR 3/7 cells. Statistical analysis (mean ± SEM) using ordinary one-way ANOVA with Tukey correction for multiple comparisons. $p < 0.001$ (***), $p < 0.0001$ (****). $N = 3$. One representative of three similar experiments is shown.

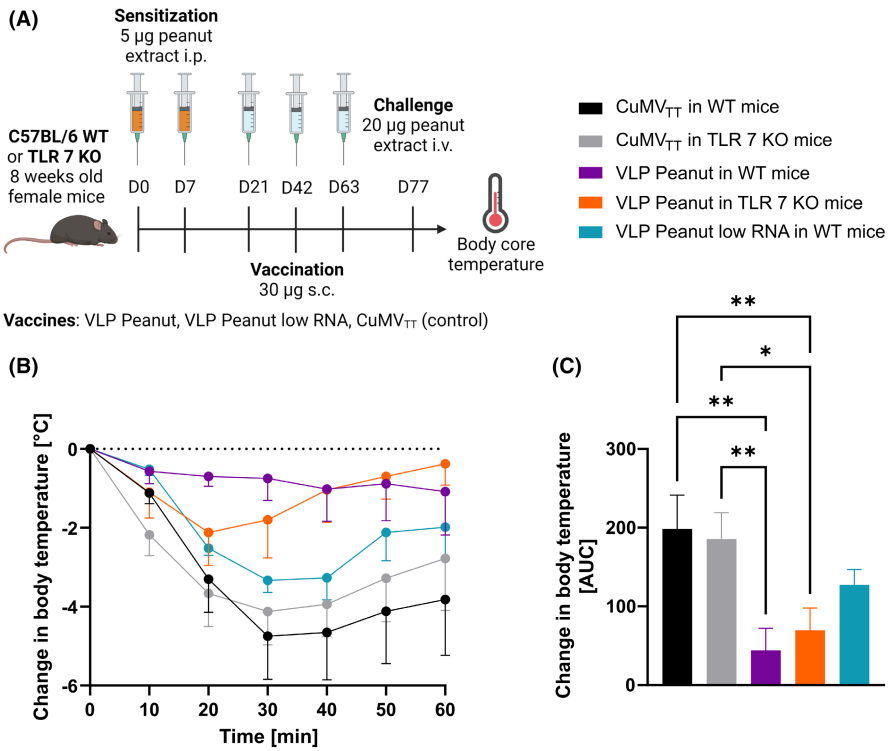

FIGURE 4 VLP Peanut-mediated protection from anaphylaxis depends on encapsulated RNA. (A) Mouse anaphylaxis model for the assessment of systemic protection after vaccination, scheme created with BioRender.com. (B) Change in body core temperature of vaccinated mice after challenge with 20 µg whole peanut extract given i.v. Last observation carried forward for mice that fulfilled the termination criterion of 6°C body temperature reduction. (C) Area under the curve (AUC) relative to baseline at 0°C depicted (B). Statistical analysis (mean ± SEM) using ordinary one-way ANOVA with Tukey correction for multiple comparisons. $p < 0.05$ (*), $p < 0.01$ (**). $N = 6$ for CuMV$_{TT}$, VLP Peanut, VLP Peanut low RNA, and $N = 5$ for CuMV$_{TT}$ TLR 7 KO, VLP Peanut TLR 7 KO. One representative of two similar experiments is shown.

s.c. with 30 µg VLP Peanut, VLP Peanut low RNA or CuMV$_{TT}$. Two booster injections with the same dose in intervals of 21 days were performed before mice were challenged by injecting 20 µg peanut extract i.v. 14 days after the last boost. Body core temperature was measured rectally for 1 h in intervals of 10 min (Figure 4A). A sharp drop in body core temperature, indicative for severe anaphylaxis, was observed in CuMV$_{TT}$ control immunized WT and TLR 7 KO mice. VLP Peanut low RNA immunized mice were only slightly protected from severe anaphylaxis compared to control mice. In contrast, VLP Peanut immunized WT mice were free of systemic reactions after the i.v. provocation with the peanut extract. Interestingly, the body core temperature of VLP Peanut immunized TLR 7 KO mice initially decreased slightly, but then recovered rapidly reaching normal levels after 40 min (Figure 4B,C). Thus, VLP Peanut vaccination mediates protection from severe anaphylaxis, thereby TLR 7 signaling seems to play a partial role, compatible with the observed robust antibody responses in the absence of TLR 7. In contrast, low RNA incorporation rates dramatically worsened the

protective capacity of the VLP Peanut vaccine underlining the role of incorporated RNA for vaccine potency.

3.5 | Determination of the Ara h 2 antigen density of VLP Peanut

As was previously shown, the optimal activation of B cells depends on the spacing between antigens on the viral surface. Antigen spacing is thereby indirectly proportional to the antigen density on the surface of the particles.[3,4,10] Since VLPs strongly resemble viruses in their surface structure, we investigated the Ara h 2 antigen density of different VLP Peanut batches with regard to their immunogenicity. These batches mainly differ in their production conditions and batch size. The Ara h 2 antigen density was first determined by SDS-PAGE analysis. For this purpose, 15 µg of different VLP Peanut batches were loaded and the signal intensities of $CuMV_{TT}$-Ara h 2 (45 kDa) and $CuMV_{TT}$ (25 kDa) derived protein bands were quantified with FIJI Image J software. Measured protein band intensities for $CuMV_{TT}$-Ara h 2 were divided by protein band intensities for $CuMV_{TT}$ of the same sample. The obtained quotient was corrected for the different molar masses and multiplied by 180, the total number of subunits in VLP Peanut. One subunit is thereby being either the unmodified $CuMV_{TT}$ or the modified $CuMV_{TT}$-Ara h 2 protein.[3] The number of Ara h 2 antigens displayed per VLP varied between 9 (batch 3) and 23 (batch 5). No Ara h 2 antigen-derived signal was observed in the $CuMV_{TT}$ control sample (Figure 5A,B). A more precise quantification of Ara h 2 antigen density was performed by mass spectrometry. To this end, two isotope labelled peptides specific for the $CuMV_{TT}$-carrier as well as one isotope labelled peptide specific for the Ara h 2 antigen were included in the analysis as internal standards. Tandem mass spectrometry was operated in targeting mode and the endogenous peptide quantification was done by one-point calibration using the isotope labelled peptides that were spiked in. Measured numbers of Ara h 2 antigen were normalized to the $CuMV_{TT}$-carrier (Figure 5C) and converted into antigen density per VLP (Figure 5D) based on the fact that VLP Peanut consists of 180 subunits.[3] VLP Peanut batches displayed an average between 7 (batch 3) and 22 (batch 5) Ara h 2 antigens per VLP (Figure 5D). Interestingly, Ara h 2 antigen densities determined by mass spectrometry highly correlate with the results obtained by

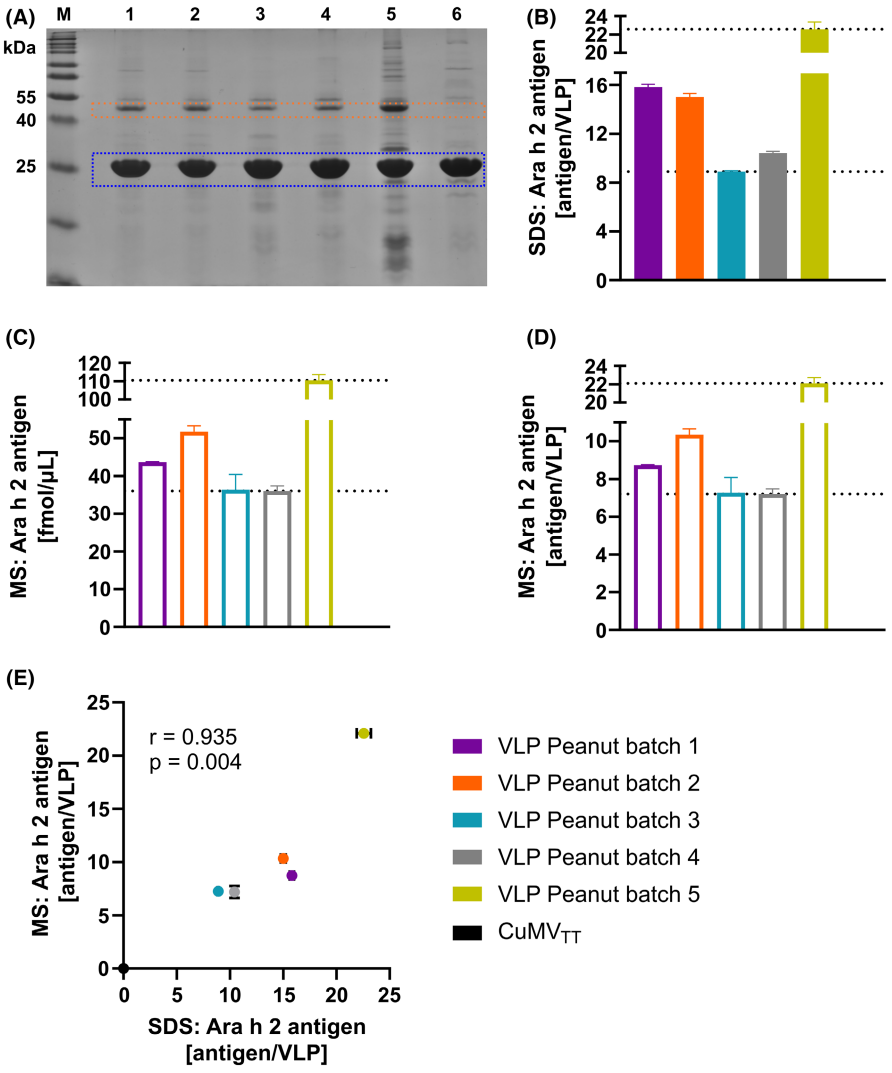

FIGURE 5 Determination of the Ara h 2 antigen density of VLP Peanut. (A) 12% SDS-PAGE of M. Protein marker, 1–5. VLP Peanut batch 1–5, 6. $CuMV_{TT}$. $CuMV_{TT}$-Ara h 2-derived protein bands are circled in orange, $CuMV_{TT}$-derived protein bands in dark blue. (B) Ara h 2 antigen density of VLP Peanut batches determined by SDS-PAGE (A) and FIJI ImageJ software analysis of $CuMV_{TT}$-Ara h 2 and $CuMV_{TT}$ derived protein band intensities. (C and D) Ara h 2 antigen density of VLP Peanut batches determined by mass spectrometry (MS). Measured peptide concentrations for Ara h 2 were normalized to both peptides specific for the $CuMV_{TT}$ backbone ($N = 2$). (E) Correlation of Ara h 2 antigen density of VLP Peanut determined by mass spectrometry and SDS-PAGE. r: Pearson correlation coefficient. p: statistical significance. Data depicted as mean ± SEM. $N = 3$ for SDS-PAGE. One representative of three similar experiments is shown for SDS-PAGE, one representative of two similar experiments is shown for mass spectrometry.

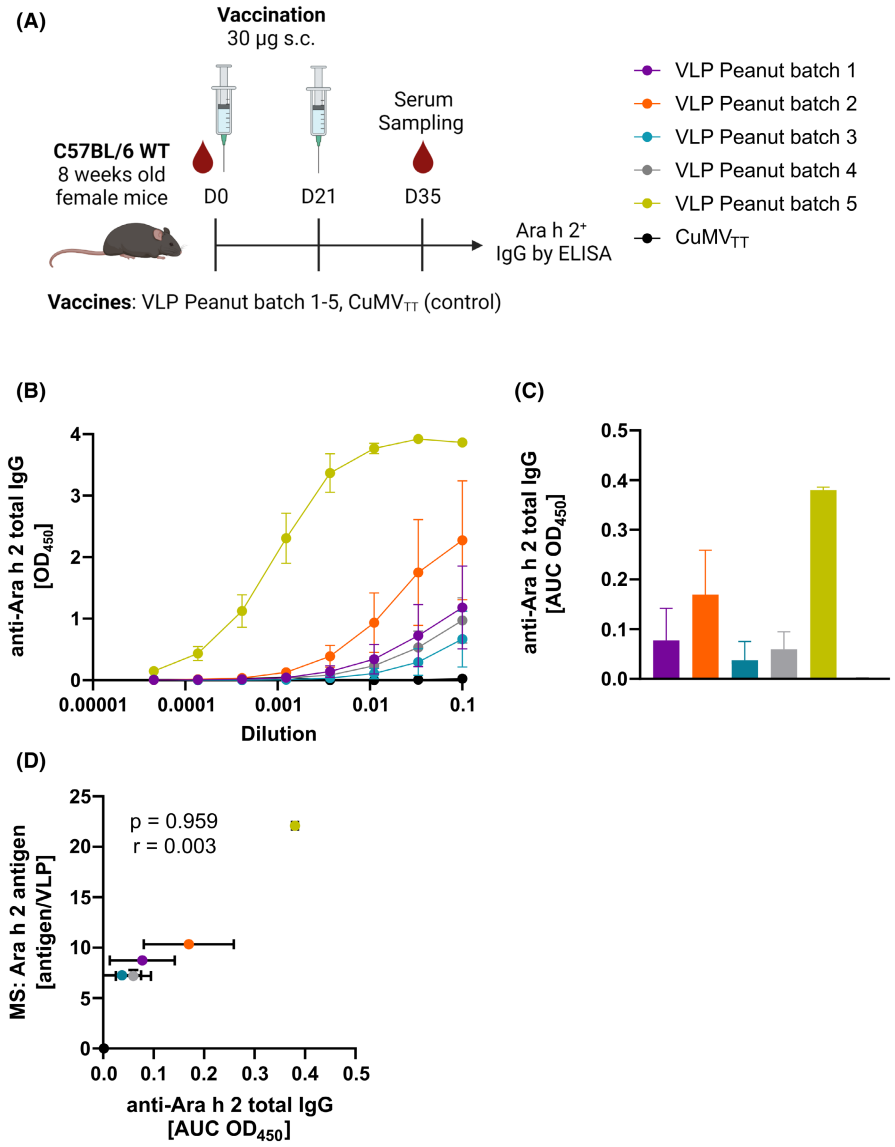

FIGURE 6 Increased Ara h 2 antigen density improves immunogenicity of VLP Peanut. (A) Vaccination regimen and bleeding schedule, scheme created with BioRender.com. (B) Ara h 2 specific serum IgG at D35 after immunization with different VLP Peanut batches measured by ELISA, OD_{450} shown. (C) Area under the curve (AUC) depicted in (B). (D) Correlation of Ara h 2-specific serum IgG at D35 with average Ara h 2 antigens per VLP quantified by mass spectrometry. r: Pearson correlation coefficient, p statistical significance. Data depicted as mean ± SEM. $N = 4$ for VLP Peanut batch 2, $CuMV_{TT}$ control, and $N = 5$ for VLP Peanut batch 1, 3–5. One representative of two similar experiments is shown.

SDS-PAGE (Figure 5E; Pearson correlation coefficient $r = 0.935$, $p = 0.004$). Consequently, Ara h 2 antigen density can be determined either by SDS-PAGE or by mass spectrometry.

3.6 | Calculating average Ara h 2 antigen distance on VLP Peanut

Based on the Ara h 2 antigen density quantified by mass spectrometry, which is 22 for batch 5 (Figure 5D) and the average diameter of VLP Peanut determined by DLS, which is 36 nm (Figure 1B), we estimated the average distance from one Ara h 2 antigen to the next on the surface of a representative VLP Peanut batch (batch 5). To this end, we approximated VLP Peanut as a sphere with a radius of 18 nm and the corresponding surface of $4 \times \pi \times 18^2 = 4072\,nm^2$ (Surface of sphere $= 4 \times \pi \times r^2$). Under the assumption, that Ara h 2 antigens are rigidly structured and equally distributed on the VLP Peanut surface, each antigen covers an area $S_a = 4072\,nm^2/22$ (measured antigen per VLP for batch 5) (Figure S2A,B). The average Ara h 2 antigen distance on VLP Peanut batch 5 calculated in this way is 14 nm (Figure S2C), which is a suitable distance for B cell activation.[10]

3.7 | Increased Ara h 2 antigen density improves immunogenicity of VLP Peanut

To compare the immunogenicity of different VLP Peanut batches, mice were immunized s.c. with 30 µg on Day 0 and 21. Before prime (D0) and 14 days after the boost (D35) serum was collected and Ara h 2 specific total IgG was determined by ELISA (Figure 6A, Figure S1C). Since some VLP Peanut batches induced suboptimal Ara h 2 specific IgG responses OD50 titers could not be determined for all batches (Figure 6B). Consequently, we assessed the area under the OD_{450}-curves depicted in Figure 6B as a measure for the Ara h 2 specific IgG response (Figure 6C). Interestingly, an increased Ara h 2 antigen density on VLP Peanut highly correlated (Pearson correlation coefficient $r = 0.959$, $p = 0.003$) with an increased Ara h 2 specific IgG response as depicted in Figure 6D. A similar icosahedral shape of particles and

negligible RNA content variation was seen in all batches of the examined VLP Peanut vaccine (Figure S3a–c, TEM of batch 5 in Figure 1B). Therefore, we assume the observed effect on the vaccine immunogenicity is solely based on the difference of Ara h 2 antigens displayed on the VLP Peanut particle's surface.

4 | DISCUSSION

Expression host-derived negatively charged RNA is the main driving force for VLP assembly and stabilizes particles once they are formed.[11] Here, we significantly reduced the prokaryotic RNA content of VLP Peanut by half without compromising VLP integrity. Complete RNA digestion was attempted but resulted in unstable particles that could not be included in the study.

In line with previous studies, we observed a TLR 7 dependent formation of high-avidity IgG as well as of IgG 1/2c subclass antibodies specific for the Ara h 2 antigen.[17-19,22] However, the total amount of Ara h 2 specific IgG antibodies was not affected by TLR 7 signaling. This seems to contradict previous findings by us and others which report lower IgG titers in the absence of a TLR 7 signal after immunization with Fel d 1 coupled to Qb-VLP or immunization with attenuated rabies virus.[22,39] The mentioned studies used a single dosage of the vaccine, whereas in the study that is being presented here, mice were given three doses of vaccine before serum antibody titers were examined. So, at least in terms of the overall quantity of produced IgG antibodies, several booster injections can compensate for a deficiency in TLR 7 signaling. Reducing the RNA content of VLP Peanut resulted in a compelling loss of Ara h 2 specific IgG antibodies after vaccination. Thereby, not only the total amount of formed IgG antibodies was affected, but also IgG subclasses and the number of high-avidity IgG antibodies. The fact that VLP-carried RNA stimulates TLR 3 and 7 to the same degrees may explain why VLP Peanut is immunogenic despite lacking a TLR 7 signal but its immunogenicity potential decreases when the carried RNA is reduced. Our data highlight the role of RNA contained in VLP Peanut as a natural adjuvant that enhances the immunogenicity of the vaccine.

VLP Peanut particles form in the cytosol of the *E. coli* expression system and therefore encapsulate predominantly prokaryotic mRNA.[3] Prokaryotic mRNA, in contrast to eukaryotic mRNA or prokaryotic tRNA, possesses no nucleoside modifications. Modified RNA nucleosides such as N6-methyladenosine, 5-methylcytidine, or pseudouridine inhibit TLR 7 stimulation reducing the associated DC activation as previously shown.[40,41] Furthermore, 2'-O-methyled nucleosides ordinary present in prokaryotic and eukaryotic tRNA prevent endosomal TLR recognition.[42] In this context, we demonstrated that only prokaryotic RNA packaged into VLPs, but not eukaryotic mRNA or prokaryotic tRNA, can stimulate TLR 7 and thus promote the production of protective IgG subclasses.[43] Thus, nucleoside modifications act as another molecular characteristic that enables the immune system to discriminate between self and foreign. Consequently, not only the amount but also the type of the encapsulated RNA influences the immunogenicity of VLP-based vaccines, which is to consider when selecting a suitable expression system host.

Interestingly, $CuMV_{TT}$-carrier specific IgG immune responses revealed no dependency on TLR 7 signaling nor the RNA content of VLP Peanut respectively. Thus, there seems to be a different dependency on the VLP-carried RNA between antigen- and carrier-specific immune responses. Additionally, we discovered that high-avidity IgG antibodies specific for Ara h 2 were four times more prevalent than high-avidity IgG antibodies specific for the $CuMV_{TT}$-carrier. The observation that VLP-specific antibodies were less dependent on TLR signaling than Ara h 2 specific antibodies may be explained by the fact that the $CuMV_{TT}$ subunits are more densely packed at a lower distance than the Ara h 2 molecules, overcoming TLR dependence. This indicates that the overall IgG response is dictated by a two-dimensional integral of TLR stimulation and antigen density. The observed differences in avidity may have structural reasons, or the less densely packed Ara h 2 molecules may be better at selecting high affinity antibodies.

We have previously demonstrated in mice that VLP Peanut induced protection from anaphylaxis is mediated via the vaccine induced anti-Ara h 2 IgG antibodies. Ara h 2 specific IgG antibodies compete with IgE for the allergen, promote IgE internalization by mast cells and engage the inhibitory receptor FcγRIIb on mast cells and basophils.[23,25-27] In the present study, we observed mild anaphylaxis in VLP Peanut vaccinated mice lacking the TLR 7 receptor and moderate to strong anaphylaxis in WT mice that received the VLP Peanut low RNA vaccine. VLP Peanut immunized WT mice were protected from anaphylaxis whereas CuMVTT control immunized mice were not. The mild anaphylaxis observed in the absence of TLR 7 might be a direct consequence of the slightly reduced amount of high-avidity IgG antibodies and/or the decreased IgG2c titers specific for Ara h 2. We have previously shown, however, that IgG subclasses play a minor role in FcγRIIb-engagement.[23] High-avidity IgG antibodies have already been associated with improved protectivity in humans against SARS-CoV-2[44,45] or Dengue virus.[46] Increased IgG2a titers, the analogue subclass of IgG2c in BALB/c mice, correlated with better protection against anaphylaxis caused by phospholipase A2 (PLA2), the major allergen of bee venom.[47,48] Interestingly, TLR 7 receptor engagement with R484 (resiquimod) or AZD8848 led to a beneficial outcome in epicutaneous immunotherapy for birch pollen-induced asthma in mice, reduced responsiveness to allergen in patients suffering from allergic rhinitis respectively.[49,50] The weak Ara h 2 specific IgG immune responses induced by VLP low RNA were reflected by the moderate to severe anaphylaxis observed in this group, confirming the important role of IgG antibodies for anaphylaxis prevention.[23,26,27] Hence, our data suggest a direct link between the RNA content of VLP Peanut and its capacity to induce IgG antibodies and mediate protection from anaphylactic reactions.

VLP Peanut is a mosaic particle consisting of $CuMV_{TT}$ and $CuMV_{TT}$-Ara h 2 proteins. The advantage of mosaic VLPs is that their structure is less affected by the size and shape of the fusion product compared to non-mosaic particles.[51] However, depending on factors like promoter strength, expression system, and

level of production, mosaic VLPs may show various rates of integration of the antigen-carrying fusion product as demonstrated by RTS,S mosaic vaccine against malaria.[52] Here, we established a mass spectrometry-based analytic method to screen the number of incorporated $CuMV_{TT}$-Ara h 2 proteins for VLP Peanut and enable a tertiary analysis of this data to estimate the average distance of Ara h 2 on the surface of the VLP, providing valuable first structural insights of the mosaic VLP. In addition, we presented with SDS-PAGE a cost-effective and easy-to-use method for the assessment of the $CuMV_{TT}$-Ara h 2 incorporation rate into VLP Peanut. We observed a strong correlation between the Ara h 2 antigen density ($CuMV_{TT}$-Ara h 2 incorporation rate) of VLP Peanut and the induced Ara h 2 specific serum IgG response. Increased antigen density, which is equivalent to a reduction in antigen spacing on the surface of the particle, facilitates BCR cross-linking leading to enhanced B cell activation and antibody responses. Our findings confirm that IgG antibody responses are regulated by epitope density of the antigen, among other factors.[10,53,54] Similar observations were recently reported by others, who observed a strong correlation between the formation of erythrocyte-specific alloantibodies and the corresponding antigen density on erythrocytes.[55]

Here, we demonstrate that VLP Peanut vaccine potency is highly dependent on the amount of Ara h 2 antigens displayed on the particle's surface as well as on the amount of VLP Peanut-carried prokaryotic RNA acting as TLR 3 and 7 ligand. Antigen density and RNA content are two parameters providing key information about the immunogenicity/protective capacity of the vaccine after manufacturing without the need for time-consuming and costly animal experiments. Antigen density and RNA incorporation may also be interesting variables to consider when optimizing new or existing VLP-based vaccines.

AUTHOR CONTRIBUTIONS

Pascal S. Krenger, Thalia L.C. Velazquez, Matthew D. Heath, Andris Zeltins, and Martin F. Bachmann were involved in design of experiments. Pascal S. Krenger, Thalia L.C. Velazquez, Matthew D. Heath, Andris Zeltins, and Martin F. Bachmann were involved in methodology. Pascal S. Krenger, Romano Josi, Jan Sobczak, Ina Balke, Matthew D. Heath, Andris Zeltins, and Martin F. Bachmann were involved in acquisition of data, interpretation, and analysis of data. Pascal S. Krenger, Thalia L.C. Velazquez, Murray A. Skinner, Callum J. W. Scott, Simon Hewings, Matthias F. Kramer, Matthew D. Heath, and Martin F. Bachmann were involved in writing, revising, and editing the manuscript. Thalia L.C. Velazquez, Ina Balke, Matthew D. Heath, and Andris Zeltins were involved in technical, material, and tool support. Martin F. Bachmann and MH were involved in study supervision. All authors read and approved the final manuscript.

ACKNOWLEDGEMENTS

We acknowledge Aleksandra Nonic and Marianne Zwicker for their technical assistance. Open access funding provided by Universitat Bern.

FUNDING INFORMATION

This publication was funded by the Swiss National Science Foundation (SNF grant 310030_185114) and Allergy Therapeutics Plc.

CONFLICT OF INTEREST STATEMENT

TCV, MS, CJWS, SH, MK, and MH are all employees of Allergy Therapeutics Plc (ATLp) which develops and manufactures immunotherapies and diagnostics including VLP Peanut. MB is under consultancy agreements with ATLp. MB is a co-founder of Saiba AG which has out-licensed vaccine development of $CuMV_{TT}$ to ATLp within allergy and other disease indications. The remaining authors declare that the research was conducted in the absence of any commercial or financial relationships that could be construed as a potential conflict of interest.

DATA AVAILABILITY STATEMENT

The data that support the findings of this study are available from the corresponding author upon reasonable request.

ORCID

Pascal S. Krenger https://orcid.org/0009-0008-7074-3842
Jan Sobczak https://orcid.org/0000-0002-5271-7826
Ina Balke https://orcid.org/0000-0002-5171-7744
Matthias F. Kramer https://orcid.org/0000-0002-3740-4733
Matthew D. Heath https://orcid.org/0000-0002-6095-4098
Martin F. Bachmann https://orcid.org/0000-0003-4370-2099

REFERENCES

1. Jennings GT, Bachmann MF. The coming of age of virus-like particle vaccines. *Biol Chem*. 2008;389:521-536.
2. Mohsen MO, Zha L, Cabral-Miranda G, Bachmann MF. Major findings and recent advances in virus–like particle (VLP)-based vaccines. *Semin Immunol*. 2017;34:123-132.
3. Bachmann MF, Jennings GT. Vaccine delivery: a matter of size, geometry, kinetics and molecular patterns. *Nat Rev Immunol*. 2010;10:787-796.
4. Bachmann MF, Zinkernagel RM. Neutralizing Antiviral. *Annu Rev Immunol*. 1997;15:235-270.
5. Baron S. Goldman Armond, P. B. Medical Microbiology. 1996.
6. Mohsen MO, Augusto G, Bachmann MF. The 3Ds in virus-like particle based-vaccines: "design, delivery and dynamics". *Immunol Rev*. 2020;296:155-168.
7. Hinton HJ, Jegerlehner A, Bachmann MF. Pattern recognition by B cells: the role of antigen repetitiveness versus toll-like receptors. *Curr Top Microbiol Immunol*. 2008;319:1-15.
8. Link A, Zabel F, Schnetzler Y, Titz A, Brombacher F, Bachmann MF. Innate immunity mediates follicular transport of particulate but not soluble protein antigen. *J Immunol*. 2012;188:3724-3733.
9. Ochsenbein AF, Fehr T, Lutz C, et al. Control of early viral and bacterial distribution and disease by natural antibodies. *Science*. 1999;286:2156-2159.
10. Vogelstein B, Dzintis RZ, Dintzis HM. Specific cellular stimulation in the primary immune response: a quantized model. *Proc Natl Acad Sci U S A*. 1982;79:395-399.
11. Perlmutter JD, Hagan MF. Mechanisms of virus assembly. *Annu Rev Phys Chem*. 2015;66:217-239.
12. Newman M, Chua PK, Tang F-M, Su P-Y, Shih C. Testing an electrostatic interaction hypothesis of hepatitis B virus capsid stability

by using an In vitro capsid disassembly/reassembly system. *J Virol*. 2009;83:10616-10626.
13. Zeltins A. Construction and characterization of virus-like particles: a review. *Mol Biotechnol*. 2013;53:92-107.
14. Janeway CA. Approaching the asymptote? Evolution and revolution in immunology. *Cold Spring Harb Symp Quant Biol*. 1989;54:1-13.
15. O'Neill LAJ, Golenbock D, Bowie AG. The history of toll-like receptors-redefining innate immunity. *Nat Rev Immunol*. 2013;13:453-460.
16. Janeway CA, Medzhitov R. Innate immune recognition. *Annu Rev Immunol*. 2002;20:197-216.
17. Hou B, Saudan P, Ott G, et al. Selective utilization of toll-like receptor and Myd88 signaling in B cells for enhancement of the antiviral germinal center response. *Immunity*. 2011;34:375-384.
18. Jegerlehner A, Maurer P, Bessa J, Hinton HJ, Kopf M, Bachmann MF. TLR9 signaling in B cells determines class switch recombination to IgG2a. *J Immunol*. 2007;178:2415-2420.
19. Krueger CC, Thoms F, Keller E, Leoratti FMS, Vogel M, Bachmann MF. RNA and toll-like receptor 7 license the generation of superior secondary plasma cells at multiple levels in a B cell intrinsic fashion. *Front Immunol*. 2019;10:1-13.
20. Tian M, Hua Z, Hong S, et al. B cell–intrinsic MyD88 signaling promotes initial cell proliferation and differentiation to enhance the germinal center response to a virus-like particle. *J Immunol*. 2018;200:937-948.
21. Castiblanco DP, Maul RW, Knode LMR, Gearhart PJ. Co-stimulation of BCR and toll-like receptor 7 increases somatic hypermutation, memory B cell formation, and secondary antibody response to protein antigen. *Front Immunol*. 2017;8:1-9.
22. Chang X, Krenger P, Krueger CC, et al. TLR7 signaling shapes and maintains antibody diversity upon virus-like particle immunization. *Front Immunol*. 2022;12:1-13.
23. Storni F, Zeltins A, Balke I, et al. Vaccine against peanut allergy based on engineered virus-like particles displaying single major peanut allergens. *J Allergy Clin Immunol*. 2020;145:1240-1253.e3.
24. Zeltins A, West J, Zabel F, et al. Incorporation of tetanus-epitope into virus-like particles achieves vaccine responses even in older recipients in models of psoriasis, Alzheimer's and cat allergy. *NPJ Vaccines*. 2017;2:1-12.
25. Sobczak JM, Krenger PS, Storni F, et al. The next generation virus-like particle platform for the treatment of peanut allergy. *Allergy*. 2023;78(7):1980-1996.
26. Uermösi C, Zabel F, Manolova V, et al. IgG-mediated down-regulation of IgE bound to mast cells: a potential novel mechanism of allergen-specific desensitization. *Allergy*. 2014;69:338-347.
27. Storni F, Cabral-Miranda G, Roesti E, et al. A single monoclonal antibody against the Peanut allergen Ara h 2 protects against systemic and local Peanut allergy. *Int Arch Allergy Immunol*. 2020;181:334-341.
28. Engeroff P, Caviezel F, Storni F, Thoms F, Vogel M, Bachmann MF. Allergens displayed on virus-like particles are highly immunogenic but fail to activate human mast cells. *Allergy*. 2018;73:341-349.
29. Abràmoff MD, Magalhães PJ, Ram SJ. Image processing with imageJ. *Biophotonics Int*. 2004;11:36-41.
30. Engeroff P, Plattner K, Storni F, et al. Glycan-specific IgG anti-IgE autoantibodies are protective against allergic anaphylaxis in a murine model. *J Allergy Clin Immunol*. 2021;147:1430-1441.
31. Wiuff C, Thorberg BM, Engvall A, Lind P. Immunochemical analyses of serum antibodies from pig herds in a salmonella non-endemic region. *Vet Microbiol*. 2002;85:69-82.
32. Türker C et al. B-fabric: the Swiss army knife for life sciences. *Adv. Database Technol. - EDBT 2010 - 13th Int. Conf. Extending Database Technol. Proc*. 2010;717-720. doi:10.1145/1739041.1739135
33. Zinkhan S, Ogrina A, Balke I, et al. The impact of size on particle drainage dynamics and antibody response. *J Control Release*. 2021;331:296-308.
34. Pasare C, Medzhitov R. Toll-like receptors: linking innate and adaptive immunity. *Microbes Infect*. 2004;6:1382-1387.
35. Browne EP. Regulation of B-cell responses by toll-like receptors. *Immunology*. 2012;136:370-379.
36. Marshall-Clarke S, Downes JE, Haga IR, et al. Polyinosinic acid is a ligand for toll-like receptor 3. *J Biol Chem*. 2007;282:24759-24766.
37. Fleischer DM, Conover-Walker MK, Christie L, Burks AW, Wood RA. The natural progression of peanut allergy: resolution and the possibility of recurrence. *J Allergy Clin Immunol*. 2003;112:183-189.
38. Bosack RC, Lieblich S. Anesthesia Complications in the Dental Office. In: *Anesthesia Complications in the Dental Office*. 2015;1-346. doi:10.1002/9781119053231
39. Luo Z, Li Y, Zhou M, et al. Toll-like receptor 7 enhances rabies virus-induced humoral immunity by facilitating the formation of germinal centers. *Front Immunol*. 2019;10:1-12.
40. Karikó K, Buckstein M, Ni H, Weissman D. Suppression of RNA recognition by toll-like receptors: the impact of nucleoside modification and the evolutionary origin of RNA. *Immunity*. 2005;23:165-175.
41. Freund I, Eigenbrod T, Helm M, Dalpke AH. RNA modifications modulate activation of innate toll-like receptors. *Genes (Basel)*. 2019;10:92.
42. Freund I, Buhl DK, Boutin S, et al. 2′-O-methylation within prokaryotic and eukaryotic tRNA inhibits innate immune activation by endosomal toll-like receptors but does not affect recognition of whole organisms. *RNA*. 2019;27:869-880.
43. Gomes AC, Roesti ES, El-Turabi A, Bachmann MF. Type of RNA packed in VLPs impacts IgG class switching—implications for an influenza vaccine design. *Vaccine*. 2019;7:1-13.
44. Struck F, Schreiner P, Staschik E, et al. Vaccination versus infection with SARS-CoV-2: establishment of a high avidity IgG response versus incomplete avidity maturation. *J Med Virol*. 2021;93:6765-6777.
45. Benner SE, Patel EU, Laeyendecker O, et al. SARS-CoV-2 antibody avidity responses in COVID-19 patients and convalescent plasma donors. *J Infect Dis*. 2020;222:1974-1984.
46. Puschnik A, Lau L, Cromwell EA, Balmaseda A, Zompi S, Harris E. Correlation between dengue-specific neutralizing antibodies and serum avidity in primary and secondary dengue virus 3 natural infections in humans. *PLoS Negl Trop Dis*. 2013;7:1-8.
47. Gómez JMM, Fischer S, Csaba N, et al. A protective allergy vaccine based on CpG- and protamine-containing PLGA microparticles. *Pharm Res*. 2007;24:1927-1935.
48. Dekkers G, Bentlage AEH, Stegmann TC, et al. Affinity of human IgG subclasses to mouse fc gamma receptors. *MAbs*. 2017;9:767-773.
49. Siebeneicher S, Reuter S, Krause M, et al. Epicutaneous immune modulation with bet v 1 plus R848 suppresses allergic asthma in a murine model. *Allergy*. 2014;69:328-337.
50. Greiff L, Cervin A, Ahlström-Emanuelsson C, et al. Repeated intranasal TLR7 stimulation reduces allergen responsiveness in allergic rhinitis. *Respir Res*. 2012;13:1-10.
51. Pumpens P, Renhofa R, Dishlers A, et al. The true story and advantages of RNA phage capsids as nanotools. *Intervirology*. 2016;59:74-100.
52. Cohen J, Nussenzweig V, Nussenzweig R, Vekemans J, Leach A. From the circumsporozoite protein to the RTS S/AS candidate vaccine. *Hum Vaccin*. 2010;6:90-96.
53. Jegerlehner A, Storni T, Lipowsky G, Schmid M, Pumpens P, Bachmann M F. Regulation of IgG antibody responses by epitope density and CD21-mediated costimulation. *Eur J Immunol*. 2002;32:3305-3314.

54. Bachmann MF, Rohrer UH, Kündig TM, Bürki K, Hengartner HZR. The influence of antigen organization on B cell responsiveness. *Science*. 1993;262:1448-1451.
55. Arthur CM, Patel SR, Smith NH, et al. Antigen density dictates immune responsiveness following red blood cell transfusion. *J Immunol*. 2017;198:2671-2680.

SUPPORTING INFORMATION

Additional supporting information can be found online in the Supporting Information section at the end of this article.

How to cite this article: Krenger PS, Josi R, Sobczak J, et al. Influence of antigen density and TLR ligands on preclinical efficacy of a VLP-based vaccine against peanut allergy. *Allergy*. 2023;00:1-16. doi:10.1111/all.15897